AIAA SPACE 2010 Conference & Exposition
30 August - 2 September 2010, Anaheim, California

AIAA 2010-8642

Design of a Mars Rapid Round Trip Mission

Nicola Sarzi Amade'[1]
University of Southern California, Los Angeles, CA, 90089

and

James R. Wertz[2]
Microcosm, Inc., Hawthorne, CA, 90250

The present work is divided in two parts. The first part analyzes the basic constraints of interplanetary round trip travel, and calculates an interplanetary train schedule (ITS) of missions to Mars in the general case of orbits with non-zero eccentricity and non-zero inclination. Options at high energy, which allow rapid round trip missions, are discussed. These options have important applications for human travel to Mars. The second part is about systems engineering aspects for a selected human rapid round trip mission to Mars. Such aspects are the development of a mission architecture, an assessment of the masses involved in the mission (such as the initial mass in LEO), an estimate of the necessary number of launches, and a preliminary analysis of the radiation protection requirements. It is found that for the mission profiles examined and for the opposition date of July 27th, 2018, the transfer times can be shorter by up to 6 weeks, compared to circular orbits. In contrast, for the opposition date of February 19th, 2027, the transfer times can be longer by up to 6 weeks. For the systems engineering study, a comparison between the requirements of a representative rapid round trip mission and those of three NASA Mars reference missions is made in order to understand the relative advantages and disadvantages of the alternatives. The mission has a total round trip time of 1.11 years and a stay time of 25.1 days. It starts on November 27th, 2026 and ends on January 8th, 2028. This mission is comparable to the NASA Mars reference missions in terms of practicality, number of launches, and masses involved.

Nomenclature

a	=	Semimajor axis (m)
CH4	=	Methane
d	=	Distance (m)
e	=	Eccentricity; Neper number (~2.71828)
E	=	Specific energy (m^2/s^2); Eccentric anomaly (deg)
g	=	Gravitational acceleration (m/s^2)
h	=	Specific angular momentum (m^2/s)
I_{SP}	=	Specific impulse (s)
LH2	=	Liquid Hydrogen
LOX	=	Liquid Oxygen
m	=	Mass (kg)
M	=	Mean anomaly (deg)
mT	=	Metric ton (or simply tonne) (= 1000 kg)
n	=	Mean motion (deg/s)
p	=	Semiparameter (m)
r	=	Radius (m)
R	=	Mass fraction
t	=	Time (s)

[1] Ph.D. Candidate, University Park Campus, Los Angeles, CA 90089, Student Member.
[2] President, 4940 W. 147th St., Hawthorne, CA 90250, Fellow.

T = Total mission duration (s)
V = Velocity (m/s)
V_∞ = Hyperbolic excess velocity (m/s)
W = Relative number of orbits
ϕ = Flight path angle (deg)
v = Mission anomaly (deg); True anomaly (deg);
μ = Gravitational parameter (m^3/s^2)
ω = Angular velocity (deg/s)

I. Introduction

THE work described here focuses on the analysis of the constraints that characterize a round trip mission design, and also on the development of some important system engineering aspects that are specifically critical for a rapid round trip mission to Mars. The former is a mathematical study, whereas the latter is an engineering study. There is a need to understand the basic constraints of round trip mission design because round trip missions may become more common in the future, for example thanks to the possible human exploration of Mars and to the realization of non-human missions involving round trips, like a Mars sample return mission.

The development of the systems engineering aspects for a rapid round trip to Mars is important, because it can reveal whether a rapid round trip mission is advantageous over a traditional long duration mission approach. Aspects like the mission architecture, the mass of the launch vehicle, and the requirements for radiation shielding are important because they can indicate whether a rapid round trip approach is feasible. The choice of Mars as the destination has several reasons. First of all, Mars has an historical, social, and scientific relevance. It is relatively close to Earth, it is suitable for exploration, and it is not completely known in terms of evidence of past life. It is most likely the first planet humans will explore.

NASA has proposed its first Mars design reference mission (DRM-1) several years ago,[1] and it has released few updated versions since then. However, there has not been yet a real opportunity to realize any of those missions. The Constellation program, before its proposed cancellation, did not directly address the design of the first human mission to Mars, because it was centered on the return to the Moon mission. The current NASA plan, instead, is addressed to the development of technologies that can make the first human landed mission to Mars possible in the late 2030's. The details of such plan are still under development. Therefore, it is important to keep studying different alternatives for Mars exploration that can still be considered in the future.

Rapid round trips to Mars are defined as missions characterized both by a rapid transfer and by a short stay on the surface. These kinds of missions can be well applied to human travel. In fact, the main possible kinds of human Mars missions are: exploration, colonization, tourism, and commerce. Although the last three scenarios are much more ahead in the future, it is clear that in some cases a rapid round trip mission could be the best solution to go to Mars and back. For example, in the case of exploration, the goals are to reduce risk, especially for the first trips, conduct basic exploration, and return safely to Earth. In the case of tourism and commerce, a short duration trip may be preferred as well, since these activities would not be appealing if the stay time was too long (up to about 2.7 years for a traditional conjunction class mission). In general, fast transits are preferred since long journeys in space would imply more exposure to cosmic and solar radiation, and to the negative effects of zero-g. Thus, there is a need to both refine our knowledge of the general rules for interplanetary round trip travels, and to apply those rules to specifically guide the design of rapid round trip missions to Mars.

II. The Fundamental Constraints of Round Trip Travel

When designing a round trip mission, there are some physical constraints that need to be respected. These basic constraints were mathematically formalized by Wertz.[2,3] By applying them to the mission design, it is possible to design missions that reduce the total round trip time with nearly the same energy expenditure of a longer trip, potentially saving in costs and resources.

For some kinds of round trip missions, in fact, the reduction of time might be more advantageous than a reduction of ΔV, for example for Mars sample return missions or Mars human missions. For those cases, a reduction in total trip time would imply a reduction in the stay-time on the planet, saving in operational and support costs, and reducing risk. A sufficiently high ΔV could reduce the total time by years. For these kinds of missions, a study of the theoretical constraints involved in the round trip design becomes necessary.

Some preliminary definitions are necessary: the home planet is the planet where the round trip starts and ends, the traveler is the spacecraft that realizes the journey, and the target planet is the planet that is visited. The mission anomaly is defined as the angular position of any of the orbiting objects with respect to a fixed reference direction in

space. In this study, such direction is that of the mission's start point. This angle is different in general from the true anomaly, which is measured from a potentially changing periapsis position. The constraints, which are of general validity, are:

1. The difference in the change in mission anomaly between the traveler and the home planet must be an integral number of orbits.
2. The change in radial position must be the same for both the traveler and the home planet.
3. The change in cross-track position (i.e., perpendicularly to the orbital plane) must be the same for both the traveler and the home planet.
4. If a rendezvous or soft landing is planned, the velocity of the traveler at the end of the mission must match the velocity of the home planet.

Condition 1 is the main constraint for round trip mission design. It states that when the traveler goes back to the home planet, the difference in the mission anomalies of the planet and the traveler during the mission must be a multiple of 360°. All the above constraints must be met for any round trip mission.

A. Analytical Form of the Constraints

The mathematical form of the above constraints is presented next. The total mission duration, T, can be broken down into a series of transportation segments, t_t, and a stay on the target planet, t_S. At a minimum, there are an outbound trip, a stay on the target planet, and a return trip, represented respectively by t_{out}, t_S, and t_{return}. In general:

$$T = \sum t_i + t_S \tag{1}$$

During each segment, the traveler goes through a mission anomaly arc of magnitude $\Delta\nu_i$, which is the angular position measured from the Sun, with an average angular velocity of

$$\omega_i = \frac{\Delta\nu_i}{t_i} \tag{2}$$

The fundamental constraint for round trip travel can be written as:

$$\Delta\nu_H = \Delta\nu_{trav} + 2\pi W \tag{3}$$

where $\Delta\nu_H$ is the change in mission anomaly of the home planet, $\Delta\nu_{trav}$ is the change in mission anomaly of the traveler, and W is an integer that is ≥ 0 for outward trips (i.e., to outer planets) and ≤ 0 for inward trips (i.e., to inner planets). It represents the relative number of orbits between the home planet and the traveler. For the home planet:

$$\Delta\nu_H = \omega_H T \tag{4}$$

where T is the total round trip time, and ω_H is the average angular velocity of the home planet during that time (constant if we consider circular orbits). For the traveler:

$$\Delta\nu_{trav} = \omega_1 t_1 + \omega_2 t_2 + \ldots + \omega_k t_k = \sum \omega_i t_i + \omega_T t_S \tag{5}$$

where ω_i and t_i are the average angular rates and time of each travel segment, t_S is the stay time at the target, and ω_T is the average angular velocity of the target during that time (constant if we consider circular orbits). A dimensionless variable can be defined for convenience:

$$\omega'_i = \frac{\omega_i}{\omega_H} \tag{6}$$

As a consequence, the fundamental constraint of Eq. (3) can be rewritten as:

$$T = \frac{\Delta v_H}{\omega_H} = \frac{\Delta v_{trav}}{\omega_H} + \frac{2\pi W}{\omega_H} = \frac{\sum \omega_i t_i}{\omega_H} + \frac{\omega_T t_S}{\omega_H} + \frac{2\pi W}{\omega_H} = \\ = \sum \omega'_i \, t_i + \omega'_T \, t_S + W P_H \tag{7}$$

where P_H is the home planet sidereal period. From Eq. (1) we obtain the stay time as:

$$t_S = T - \sum t_i \tag{8}$$

By substituting Eq. (8) into Eq. (7) we finally obtain the total round trip time as:

$$T = \frac{\sum \omega'_i \, t_i - \omega'_T \sum t_i + W P_H}{1 - \omega'_T} \tag{9}$$

Specific values to use in the equations in the case of Earth-Mars missions are as follows:
ω_H ~ 0.986 deg/day; ω_T ~ 0.524 deg/day; P_H ~ 365.24 days

B. Transfers Types and Reduction in Total Round Trip Time

The fundamental problem with round trip travel is that the total time is driven by the constraint to have the home planet make an integral number of additional orbits around the Sun compared to the traveler.

As illustrated in Fig. 1, the T1, T2, T3, and T4 transfers are those transfers that are tangent either to the inner planet's orbit or to the outer planet's orbit. In particular, T1 and T3 are direct transfers, since they intersect the planets' orbits only once, whereas T2 and T4 are indirect transfers, since they intersect the planets' orbits twice.

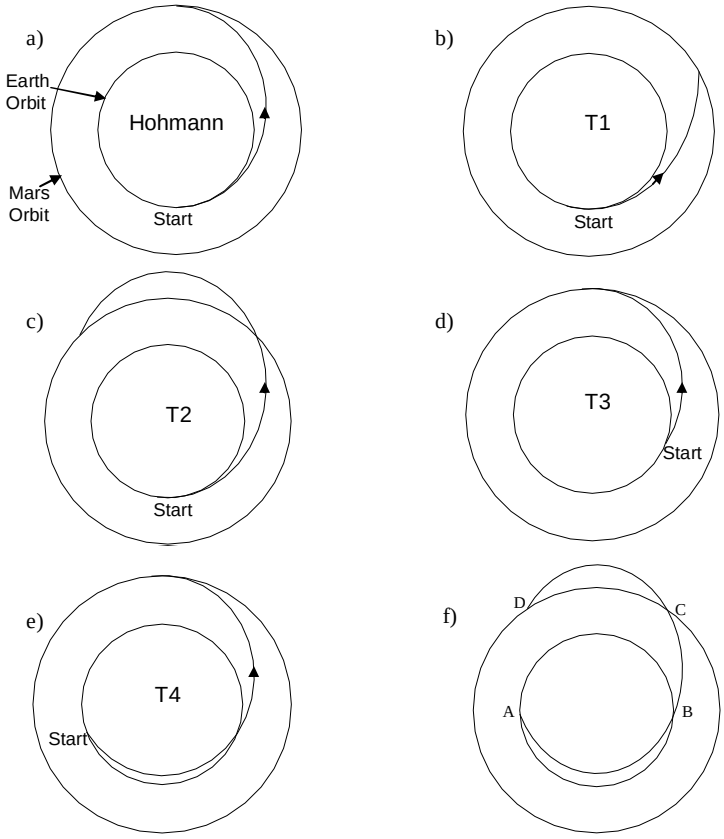

Figure 1. Different types of orbital transfers.

Additionally, T1 and T2 transfers are tangent to the inner planet's orbit, whereas T3 and T4 transfers are tangent to the outer planet's orbit. More in detail, a T1 Transfer occurs on the first half of a transfer trajectory which goes beyond the Target planet and has a mission anomaly change of less than 180°. Instead, a T2 Transfer occurs on the second half of the transfer trajectory with a mission anomaly change of more than 180°. Figure 1 also shows possible non-tangent transfer profiles (image f). In this case, the transfer arcs are not tangent to either of the planets' orbits. In particular, arc B-C is called an NT1 transfer, B-D an NT2 transfer, A-D an NT3 transfer, and A-C an NT4 transfer. These pofiles represent a more general case.

Only four impulsive thruster firings are assumed at this stage: the first to leave the Earth, the second to match Mars' orbital velocity, the third to leave Mars, and the fourth to match the Earth's velocity at the end of the return journey. The ΔV's to leave or land on the planets are not included so far.

The round trip time is driven by the need that the difference in the number of revolutions between the Earth and the traveler is an integer, *W*. As long as the value of *W* does not change, changing the 1-way travel time by adding energy has almost no impact on the total round trip time. However, if the energy is increased sufficiently, it is possible to reduce the value of *W* and create a large step reduction in the total mission duration. The duration of such step is equal to the synodic period of the home and target planets (2.135 years for the Earth and Mars). This can be seen in Fig. 2, for a T1/T1 mission profile (assuming circular coplanar orbits of the Earth and Mars).

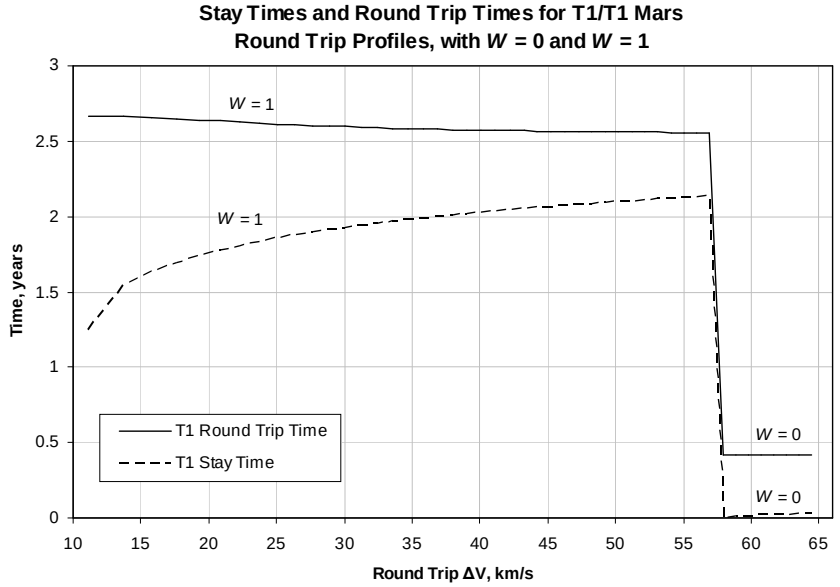

Figure 2. *W*=0 and *W*=1 direct transfer missions to Mars.

C. Round Trips with *W*=0

Round trip times are mostly driven by the value of *W*, therefore mission durations and stay times are determined primarily by the amount of ΔV that is available. Hohmann round trips to nearby objects take very long. To significantly reduce the round trip time to such locations, trips for which *W*=0 are needed, which requires considerably more energy than the Hohmann transfer. Round trip missions with *W*=0 are referred to as rapid round trips (RRT).

There are two main classes of *W*=0 missions: *W*=0 direct transfer missions and *W*=0 indirect transfer missions. *W*=0 direct transfer missions are those that use a T1 transfer to reach the target's orbit, remain there for a certain period, and then transfer back on a T1 trajectory usually equivalent to the outbound one. This type of transfer requires a total ΔV of about 6 times that of a Hohmann transfer round trip, but it allows to reduce the total round trip time from about 2.5 years to less than 6 months (although the stay time is very short). This can be mitigated by using *W*=0 indirect transfer missions, which have a T4 transfer on one or both legs, to provide a high angular velocity segment to offset the lower angular velocity at the target. Having one leg with rapid, direct transfer and one leg with an indirect transfer can provide good compromises in terms of total round trip time and required mission ΔV.

An example of indirect transfer is shown in Fig. 3, for a Mars mission with an outbound T1 transfer leg and an inbound T4 transfer leg, for both *W*=0 and *W*=1. When *W*=0, the total ΔV required is between 3 and 5 times that of a

Hohmann transfer round trip, for a total round trip time of a little more than 1 year and stay times of reasonable duration.

For W=0 round trips, the average angular speed of the home planet and that of the traveler must be the same over the entire duration of the mission. Any periods of slower angular speed on the part of the traveler, including stay time at the target, must be compensated by periods of faster angular speed in order to get back home. Equivalently, the difference in mission anomaly must be zero.

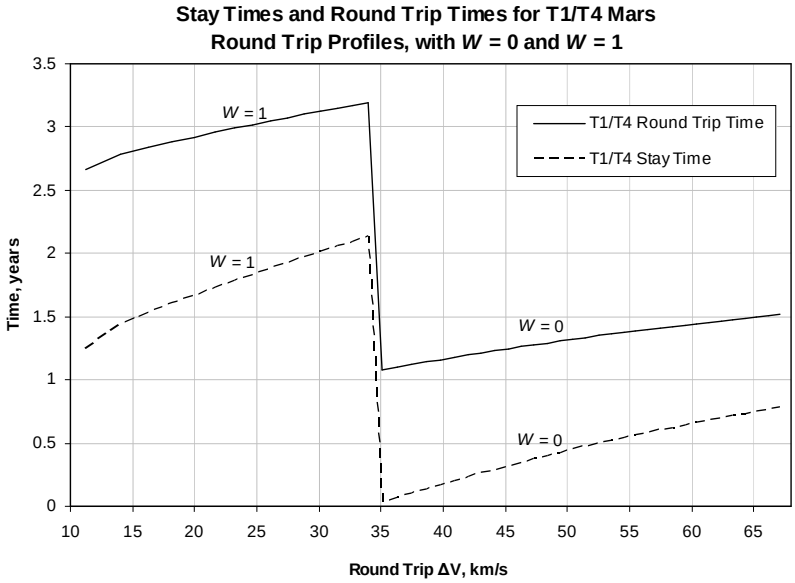

Figure 3. W=0 and W=1 indirect transfer Mars round trips. The inbound leg is inside the Earth's orbit.

III. Non-Tangent Mission Profiles

Figure 4 shows the total trip time of NT1/NT4 Earth-Mars round trips as a function of the total ΔV, for different initial (Earth departure) flight path angles (FPA's). This is a more general case because it does not require tangency to either of the planets' orits. The calculations assume that the orbits of the Earth and Mars are circular and coplanar, and that the ΔV's are only the heliocentric ones (hyperbolic escape and capture ΔV's are not considered at this point). The return trip is designed in a way that the traveler leaves Mars with the same FPA with which it arrived, changed of sign, and same ΔV (symmetric departure).

The plot shows that for a given departure FPA, the trip time decreases with total trip ΔV (except for FPA values approaching 90º). The plot also shows that as the initial flight path angle increases, both total trip time and total trip ΔV increase. Additionally, for initial FPA's between 0º and a value between 20º and 30º (not clearly identifiable in the plot but close to 25º), both trips with W=0 and W=1 are possible. For greater FPA's, only trips with W=0 are possible. When the initial FPA is 0º, the case reduces to a T1/T1 round trip. One significative result of this plot is that for FPA's greater than 0º and smaller than 40º, W=0 missions are possible at ΔV's smaller than for FPA=0º, which confirms the advantage of doing non-tangent transfers instead of tangent transfers.

The curves in Fig. 4 are limited to their left by the fact that for small enough round trip ΔV's, the departure ΔV does not result high enough to achieve the desired departure FPA. However, based on this limitation, the left extreme of the curves should extend a little bit more on the left than is shown in the plot. But there is a stronger limitation that trims off the left side of the curve even more, up to the point that is shown. This limitation is that for too small round trip ΔV's, the departure ΔV is not high enough to allow the traveler's transfer orbit to intersect Mars orbit. On the right hand side, instead, the curves are limited by the fact that for too high round trip ΔV's the departure transfer orbit becomes parabolic first, and then hyperbolic (the energy becomes positive). Since the current study is only limited to analyze elliptical transfer types, the parabolic and hyperbolic cases are not shown.

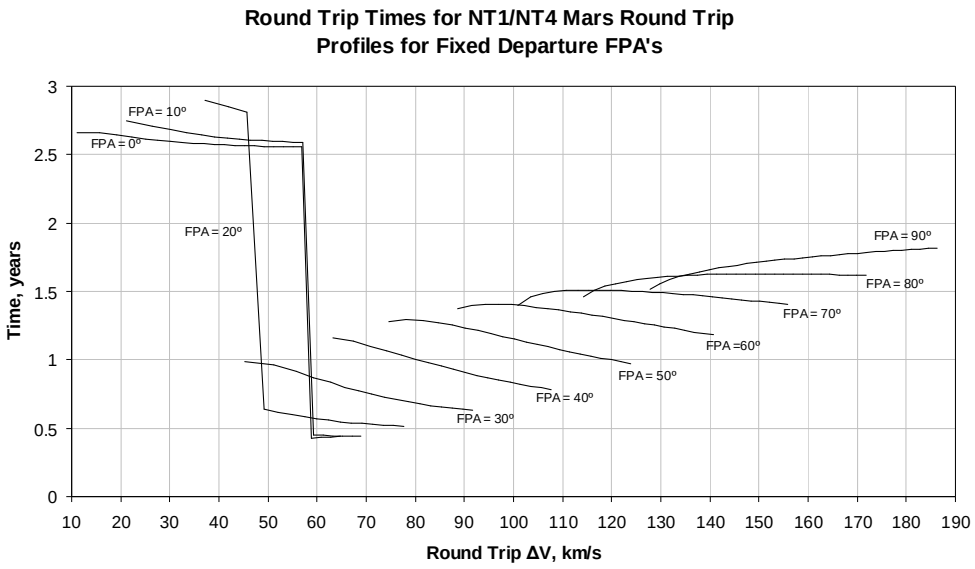

Figure 4. Total round trip time as a function of round trip Δ*V* for fixed departure flight path angles.

IV. The Interplanetary Train Schedule

An interplanetary train schedule (ITS) is a table or a plot showing departure and arrival times for various interplanetary round trips and the cost in terms of Δ*V*. For the mission segment going from the home to the target, the following relations are valid:

$$\nu_{start} = T_{start}\,\omega_H \tag{10}$$

$$\nu_{arrive} = T_{arrive}\,\omega_T \tag{11}$$

which show the relationship between the start time, T_{start}, and the start mission anomaly, ν_{start}, and between the arrival time, T_{arrive}, and the arrival mission anomaly, ν_{arrive}. These quantities are relative to when the home planet and the target planet are at opposition. Opposition reoccurs at intervals equal to the synodic period. For the traveler, we must have:

$$\Delta\nu_{transfer} = \nu_{arrive} - \nu_{start} = \omega_{transfer}\,t_{trans} \tag{12}$$

By substituting Eqs. (10) and (11) into Eq. (12), we obtain:

$$T_{start} = \frac{t_{trans}\left(\omega_T - \omega_{trans}\right)}{\omega_H - \omega_T} \tag{13}$$

$$T_{arrive} = T_{start} + t_{trans} \tag{14}$$

Equations (13) and (14) provide the required start and arrival times relative to opposition given a transfer arc $\Delta\nu_{trans}$ (from which, knowing the orbits of the planets, also a transfer time, t_{trans}, is defined). Equations (10) and (11) then provide the start and arrival mission anomalies.

The above equations can be used to construct a "train schedule" of high energy transfer times to the planets as a function of phase in the synodic period, i.e., transfer arc, and total transfer Δ*V*. The general mission design process allows us to look at the total round trip time, the stay time, and the mission start and end times relative to opposition, all as a function of the total Δ*V* available for the mission.

As the Δ*V* increases, each of the transfer types, T1 to T4, leads to a well-defined sequence of departure and arrival times that must be met or the traveler will have to wait for the next opposition, or use a higher Δ*V*. The Interplanetary Train Schedule (ITS) has this name because it provides a discrete number of departure times and arrival times, with their associated "cost".

Figure 5 shows the ΔV on the vertical axis ($V1 + V2$ on the outbound leg and $V3 + V4$ on the return leg, where $V1$, $V2$, $V3$, $V4$ are the ΔV's of the mission), and the time relative to opposition on the horizontal axis, where opposition is represented by a vertical blue line at 0. The next opposition is one synodic period later, shown by the vertical blue line on the right. For both outbound and return flights, the traveler leaves on a green line and arrives on a red line, using direct transfers. The green line on the x-axis on the left represents the range of departure times from Earth, whereas the arrival times at Mars are along the red line starting to the left of the opposition line. The green line on the right shows the departure times from Mars, and the red line on the x-axis represents the arrival at Earth corresponding to these departure times. The black lines show specific sample trips, with the mark in the center of the line showing the split between $V1/V2$ on the outbound trip, and between $V3/V4$ on the return trip. The lowest black line is the Hohmann transfer orbit, which has the lowest total ΔV (~11 km/s).

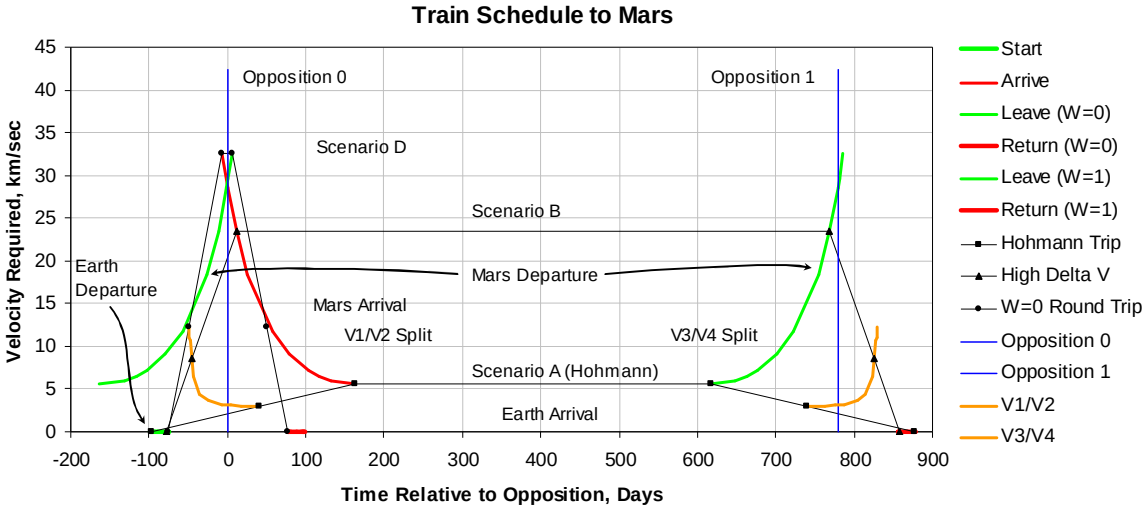

Figure 5. Interplanetary Train Schedule to Mars with transition from W=1 to W=0.

The orange line represents the locus of the ΔV split between the first and second burns on each leg of the trip. It shows on the left the $V1/V2$ split and on the right the $V3/V4$ split. On the left, $V1$ is below the orange line and $V2$ is above it. On the right, $V3$ is above the orange line and $V4$ is below it. The second ΔV on each leg which occurs at arrival can potentially be done entirely or partially by direct entry or aerobraking, rather than by use of rockets and, therefore, propellant. So, there is a potential advantage to a trip path that splits the total ΔV into a smaller amount on the departure burn and a larger amount on the arrival burn.

V. Generalization to Real Orbits

A strategy was laid out to expand the results obtained for circular coplanar orbits of the Earth and Mars to real orbits. The orbits of the Earth and Mars have of course a non-zero eccentricity and a non-zero relative inclination. When the traveler travels between the two planets, this fact must be taken into account. The round trip mission types that were chosen for the passage to real orbits are T1/T1, T1/T4, and NT1/NT4 with fixed departure ΔV, since they are particularly significative in terms of comparing the required ΔV's for the missions.

A. Orbital Elements of the Earth and Mars

The orbital parameters of the Earth and Mars at the Standard Julian Epoch (J2000) are the following:[4]

- Earth:
  - Semi-major axis: a=1.00000011 AU
  - Eccentricity: e=0.01671022
  - Inclination: i=0.00005º
  - Longitude of ascending node: Ω=348.73936º
  - Argument of perihelion: ω=114.20783º
  - Mean anomaly: M=357.51716º
  - Longitude of perihelion: $\tilde{\omega} = (\omega+\Omega) \mathrm{mod}_{360^\circ} = 102.94719^\circ$
  - Mean longitude: $L = (\tilde{\omega} + M) \mathrm{mod}_{360^\circ} = 100.46435^\circ$

- Mars:
  - Semi-major axis: a=1.52366231 AU
  - Eccentricity: e=0.09341233
  - Inclination: i=1.85061º
  - Longitude of ascending node: Ω=49.57854º
  - Argument of perihelion: ω=286.4623º
  - Mean anomaly: M=19.41248º
  - Longitude of perihelion: $\tilde{\omega}=(\omega+\Omega)\mathrm{mod}_{360º}$=336.04084º
  - Mean longitude: $L=(\tilde{\omega}+M)\mathrm{mod}_{360º}$=355.45332º

where 1 AU is equal to $1.49597870691 \cdot 10^{11}$ m, and $\mathrm{mod}_{360º}$ is the modulo function, which in general adds or subtracts multiples of 360º to the result in order to express it as a quantity between 0º and 360º. The above quantities were used in the calculations. In general, the orbital elements vary with time. However, for this study, they were considered constant for every date (except the mean anomaly). For the Earth, also, it was assumed that the semi-major axis is exactly 1 AU and the inclination is exactly 0º. These choices were considered to be good for this study, since the temporal variations of the orbital elements are in general very small.

The orbital parameters of the Earth and Mars listed above are referred to a J2000 reference system, which has the following characteristics: inertial, centered at the Sun, having the x direction coinciding with that of the Vernal Equinox at J2000, the y direction being at 90º counterclockwise from the x direction, and the z direction being perpendicular to both x and y on a right-handed triad (coinciding with the direction of the ecliptic north pole at J2000). This is indeed a fixed reference frame because it maintains the direction of the axes at epoch J2000 at any instant.

The calculations of round trip times are dependent on the selection of a particular opposition date around which the round trip occurs. The synodic cycle of the Earth and Mars is about 15 years long. This is the approximate period of time it takes for the opposition of the two planets to reoccur at nearly the same original direction in inertial space. Such period of time includes the occurrence of seven synodic periods (eight oppositions), each every about 26 months (780 days) at different directions in space. The seven synodic periods (eight oppositions) that were considered for this analysis are characterized by the following opposition dates, provided by SEDS, University of Arizona chapter, at http://seds.org/~spider/spider/Mars/marsopps.html:

1. July 27 2018, 05:07 UT
2. October 13 2020, 23:20 UT
3. December 8 2022, 05:36 UT
4. January 16 2025, 02:32 UT
5. February 19 2027, 15:45 UT
6. March 25 2029, 07:43 UT
7. May 4 2031, 11:57 UT
8. June 27 2033, 01:24 UT

These dates were chosen because they are in the relatively near future and they can be used in realistic scenarios of upcoming robotic and human missions. However, the entire analysis was done for only two opposition dates, July 27th 2018 and February 19th 2027, since they represent, respectively, the closest and farthest approach between the Earth and Mars, and all other cases fall in between these two. This is a reasonable choice, since most of the useful information comes from just analyzing the best and the worst cases.

B. Iterative Calculation Process

At first, only the eccentricity was introduced in the calculations. All the other orbital parameters were introduced later (Section D). The passage to eccentric orbits was made using a trial and error procedure. At arrival, the traveler must intersect Mars' orbit when Mars is there: as a consequence, for a given mission ΔV, the real time of departure from Earth must be found as a function of the eccentricity. The iterative procedure consists first of calculating the start date for the circular orbits case (Iteration 1). This was already done when studying circular orbits. For such approximation, different ΔV's were used for the Earth departure, starting from the minimum possible ΔV (the Hohmann transfer ΔV), and incrementing the value by 200 m/s at a time up to a ΔV for which the transfer arc passed from elliptic to parabolic. By using equations that provide start and arrival times with respect to opposition,[5] it was possible to calculate the start date of the mission for each given ΔV (still within circular orbits).

Iteration 2 introduced the eccentricity of the planets' orbits, and was used to find the actual intersection with Mars' orbit (Fig. 6). Given a precise opposition date, a transfer ΔV, and an arc type, it is not allowed anymore to depart from Earth at any time during Earth's orbit but there is only one departure point that can allow a transfer to

Mars under such conditions. The start date is unknown at first; however, thanks to the iteration process, it is possible to make a first guess considering the start date equal to the one previously found for circular orbits. This way, the intersection between the traveler and Mars' orbit will be close enough to the actual position of Mars at the instant of intersection. It is then possible to measure by how much the intersection misses the actual position of Mars, and start a new iteration (Iteration 3) with an improved start date, and repeat this process until convergence. In Fig. 6, the intersection point is indicated by a green dot and the first two approximations are indicated by an orange line and a blue line, respectively.

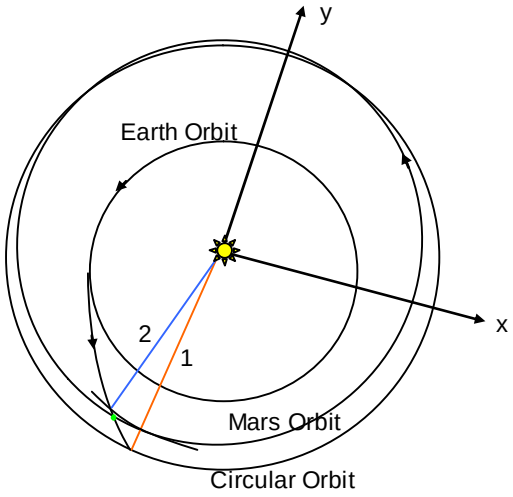

Figure 6. Iterative method used to find the intersection between the transfer orbit and Mars' orbit.

The first thing that is calculated is the intersection of the transfer orbit with a circular orbit having a radius equal to the Mars' orbit semi-major axis, a_{mars}=1.52366 AU. This produces a value of true anomaly on the transfer orbit given by:

$$\nu_{arrival} = \arccos\left(\left(\frac{p_{trans}}{r_{mars}} - 1\right) \cdot \frac{1}{e_{trans}}\right) \tag{15}$$

where for this first iteration (within Iteration 2) r_{mars}=a_{mars}. This value of true anomaly is used to find the absolute direction (ecliptic longitude) of the intersection with respect to the fixed reference frame. This direction is given by the sum of the longitude of the Earth at start date and the Δtrue anomaly of the transfer arc. By knowing this absolute direction of the intersection, it is then possible to calculate the real distance of Mars' orbit from the Sun along such direction. This distance is given by:

$$r = \frac{p_{mars}}{1 + e_{mars} \cos \nu} \tag{16}$$

where, in this case, ν is given by the difference between the absolute direction of intersection and the absolute direction of Mars' perihelion. The second iteration starts again by calculating the true anomaly of intersection, $\nu_{arrival}$, on the transfer orbit, but this time by using the new distance r just found. The iteration produces a new $\nu_{arrival}$, and a new distance r. After only few iterations of this kind, it is possible to find the value of true anomaly at intersection with an error of less than 0.1º.

Now that the true anomaly of intersection is found, the first challenge is solved. To solve the second challenge (calculating where Mars is at the instant of intersection), the procedure first consists of calculating Mars' mean anomaly at the instant of intersection. This is given by the mean anomaly at start plus the variation in mean anomaly during the transfer time. From the mean anomaly it is possible to calculate the true anomaly of Mars by applying a power series expansion.[5] Once the true anomaly is known it is compared with the true anomaly of the intersection point on Mars' orbit. In general the two true anomalies do not coincide, and Mars results to be few degrees off of the

intersection point (ahead or behind). Therefore, a 3rd category of iterations (Iteration 3) must be introduced, on the start date.

The input for the 3rd iteration is a new start date for each previously given ΔV. The new start date depends on the error in true anomaly obtained at the end of iteration 2. From the error in true anomaly, it is possible to calculate the error in terms of time between the intersection point and the actual location of Mars on its orbit. The new start date is therefore set equal to the previous start date plus a term given by the product between the time error from the end of the iteration 2 and a coefficient f, that can be tuned to minimize the error. In mathematical form:

$$(\text{Start Date})_{\text{iteration 3}} = (\text{Start Date})_{\text{iteration 2}} + f * (\Delta T_{\text{iteration 2}}) \tag{17}$$

where, at first, f can be set equal to 1. The rest of the procedure in iteration 3 is: calculation of the positions of Earth and Mars at start date, characterization of the transfer arc, calculation of the intersection point between the transfer arc and Mars' orbit, and calculation of the new time error between the intersection point and the real Mars' position. At this point, it is possible to go back and tune the value of the coefficient f, in order to minimize the time error. At the end of the iteration, the time error is reduced significantly, always below 10 minutes.

C. Results for Eccentric Orbits

A plot representing the outbound arc for T1/T1 profiles and for the opposition of July 27, 2018 has been created, and is presented in Fig. 7. This plot is based on the exact eccentricities of the Earth's and Mars' orbits, which are shown in black color. The plot also shows 3 different example transfer orbits in green: one at the smallest ΔV (6.05 km/s), one at an intermediate ΔV (17.23 km/s), and one at the maximum elliptical ΔV (29.23 km/s).

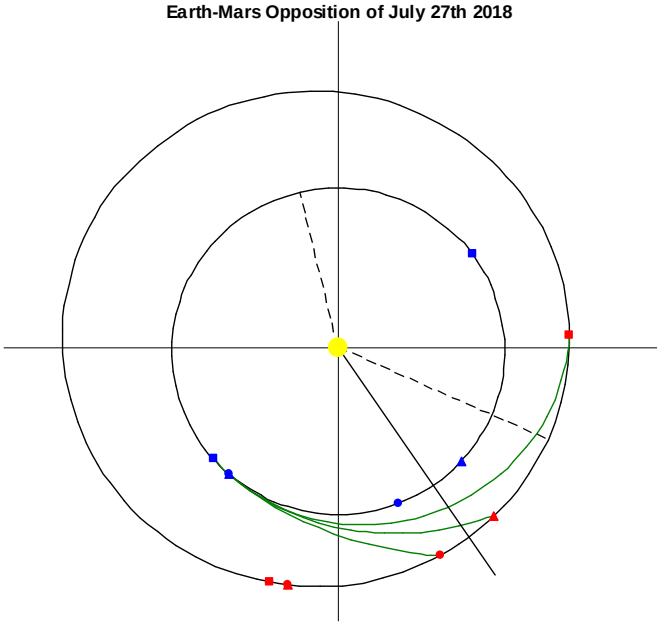

Figure 7. T1/T1 profile. Outbound journey for 3 different ΔV cases (low, medium, high).

The blue marks indicate the positions of the Earth at start date and arrival date for those three different cases, where in particular the square represents the lowest ΔV case, the triangle represents the intermediate ΔV case, and the circle represents the highest ΔV case. Similarly, the red marks represent the positions of Mars at start date and arrival date, characterized by the same mark shapes of the Earth for the three different cases. The black dotted lines represent the direction of perihelion for the Earth and Mars, and the black solid line coming out from the Sun represents the direction of opposition. It is clear from the plot that on July 27, 2018 opposition occurs relatively close to Mars' perihelion. The reference system is once again based on the direction of the Vernal Equinox at J2000, represented by the positive direction of the x-axis (pointing right). The return journey for the T1/T1 profile and for the case W=0 is instead shown in Fig. 8. Once again, three cases are shown: smallest ΔV (6.30 km/s), intermediate ΔV (15.46 km/s), and maximum elliptical ΔV (38.59 km/s). More cases are presented in Ref. 5.

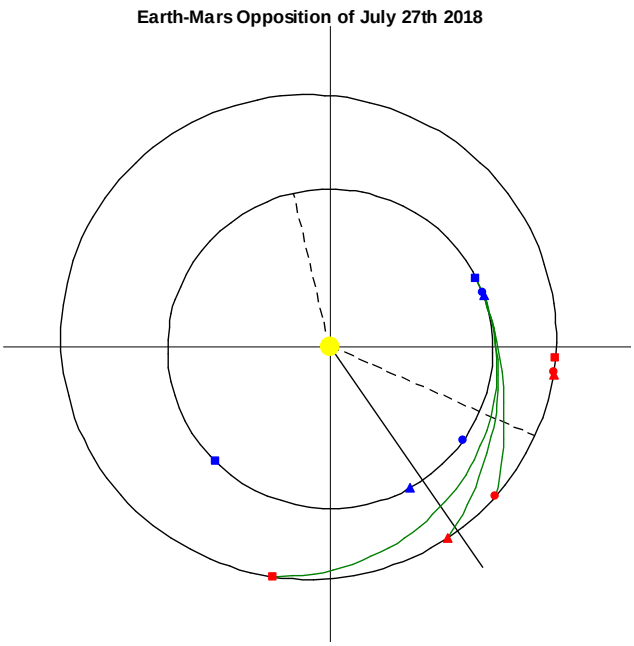

Figure 8. T1/T1 profile. Return journey for 3 different ΔV cases (low, medium, high).

D. Inclusion of the Orbital Inclination

After including the eccentricities of the orbits of the Earth and Mars, the next step was to include all other orbital elements of the planets, to improve even further the analysis of round trips. In particular, the inclination of Mars' orbit with respect to the ecliptic plane was taken into account and the actual ΔV's for Mars round trips were calculated. The passage from simple eccentric orbits of the Earth and Mars to real orbits increased the total ΔV slightly, due to the inclusion of plane changing maneuvers in heliocentric space at both outbound and return.

Mars' orbital plane has an inclination i of 1.85º with respect to the ecliptic plane. A problem of real orbits is the need to perform plane changes in a way that minimizes the propellant consumption. Spherical geometry was used to solve this problem, in particular full-sky spherical geometry, which accounts for transfer-arcs and stay-arcs that are greater than 180º (for example, some T4 transfer arcs). The orbital plane change equation valid when the geometry of the orbit does not change is the following:

$$\Delta V_i = 2V_{initial}\cos(\phi)\sin\left(\frac{\Delta i}{2}\right) \tag{18}$$

where ΔV_i is the amount of ΔV needed for plane change, Δi is the inclination change, $V_{initial}$ is the velocity at maneuver (which remains the same in value after the maneuver), and ϕ is the flight path angle at maneuver.

Given the complexity of obtaining an exact solution, some assumptions were made to simplify the problem with still acceptable results. The main assumption is that the departure and arrival dates calculated in 2D do not change. Equivalently, the transfer durations and the transfer arc lengths do not change. These assumptions are true within few hours over a 2 years mission, as was estimated analytically, so they are acceptable. Thus, the real goal of this study is simply to calculate the additional ΔV required for the plane change in heliocentric space (ΔVi).

The second assumption is that the traveler makes the inclination change in heliocentric orbit 90º before arriving to destination, which is the point where the inclination change is minimum. As a consequence, the portion of the transfer arc off the ecliptic plane (both at outbound and return) is 90º, whereas the portion on the ecliptic plane is given by the difference between the total arc length, calculated in 2D, and 90º. However, if the total transfer arc is less than 90º, then the entire transfer journey is made off the ecliptic plane, to keep the inclination change as small as possible, and in that case the arc length off the ecliptic plane is set equal to the transfer arc length calculated in 2D. When the traveler leaves a planet, it leaves it on a transfer orbit that remains on that planet's orbital plane (ecliptic plane at outbound and Mars' orbital plane at return) until it is the right time to make the plane change.

The analytical demonstration of the advantage of this strategy is the following. By using the equations of spherical geometry for right spherical triangles taken from Ref. 6, and by looking at Fig. 9, we can calculate:

$$\sin B = \frac{\sin b}{\sin h} \tag{19}$$

where *B*, *b*, and *h*, are shown in the Figure. *B* is the quantity that has to be minimized.

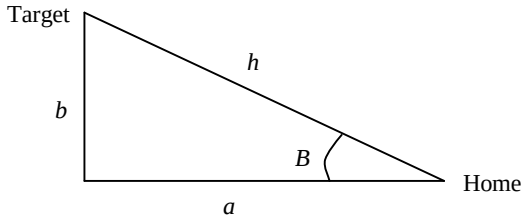

Figure 9. Right spherical triangle.

We can see that B is minimized when h=90º, since in that case the denominator on the right-hand side of Eq. (19) is maximized. By using another spherical geometry relation, we can calculate:

$$\cos a = \frac{\cos h}{\cos b} \tag{20}$$

Since h=90º, then cos(h)=0. Therefore, cos(a)=0, which means that a=90º as well. This fact can be proved also by using full-sky spherical geometry equations.

It is important to note that making the plane change 90º prior to destination (which is the point of minimum inclination change) is not necessarily the point at which the ΔVi is minimum, because as Eq. (18) shows, the ΔVi is minimized by an opportune combination of Vinitial, ϕ, and Δi. In particular, all the rest being fixed, the smaller the Vinitial (and this happens closer to apoapsis), the smaller the ΔVi. However, making the inclination change at 90º is a good approximation, and actually, since the resulting ΔVi at that point is just slightly higher than the minimum one, it ultimately gives a conservative assessment of the propellant requirements, and so it is better for the design phase.

The third major assumption that was made is that only one main inclination change per transfer was considered, for a total of two inclination changes over the whole round trip mission. In particular, only the heliocentric plane change to leave the planet (Earth at outbound and Mars at return) has been considered, whereas the one at destination (Mars at outbound and Earth at return) has not been considered, since the goal of the traveler is not to stay in heliocentric space with the same velocity of the planet, but actually to rendezvous with it and land on it. As a consequence, no constraints have been posed to the landing site, whereas constraints only exist on the launch site.

VI. Results for Real Orbits

Based on the above assumptions, the following results have been obtained. Figures 10 to 13 show the plots of round trip mission duration as a function of total mission ΔV for real orbits. Cases include T1/T1 and T1/T4 rofiles. The Figures also present the results previously obtained for eccentric orbits and circular orbits and compare them to the new, more accurate results. It is evident that the introduction of the inclination change (in blue) does not radically change the shape of the results obtained for eccentric orbits (in orange); however, the new curves are all shifted slightly towards the right-hand side, due to the higher total ΔV's. More cases are presented in Ref. 5.

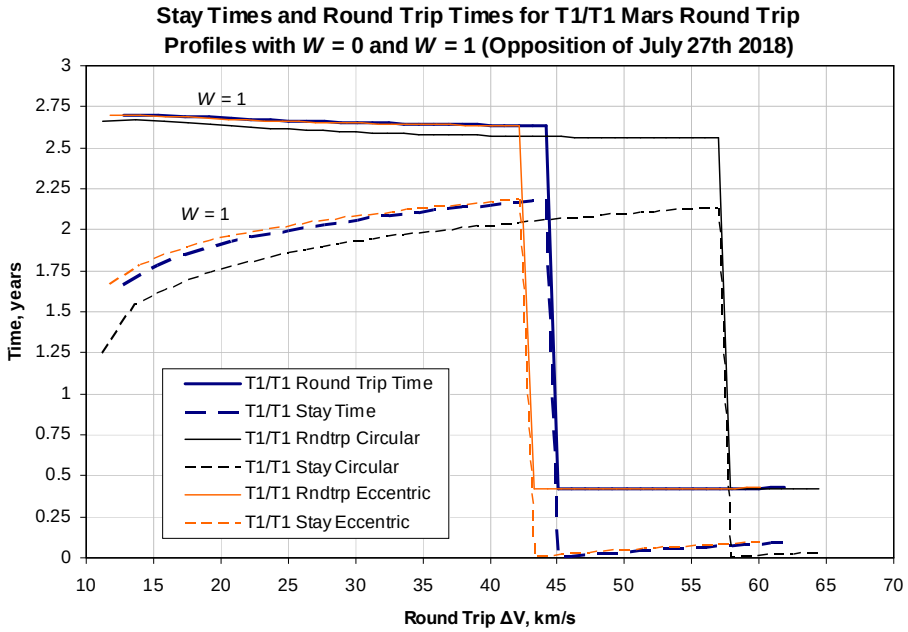

Figure 10. T1/T1 total trip and stay times as a function of the total mission Δ*V* for real orbits compared to eccentric and circular orbits. Opposition of July 27th, 2018.

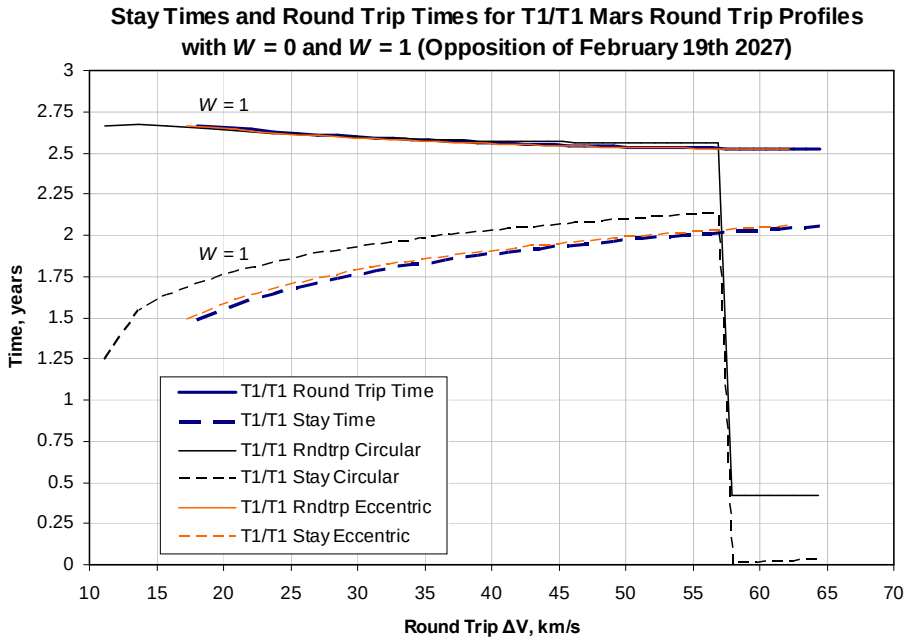

Figure 11. T1/T1 total trip and stay times as a function of the total mission Δ*V* for real orbits compared to eccentric and circular orbits. Opposition of February 19th, 2027.

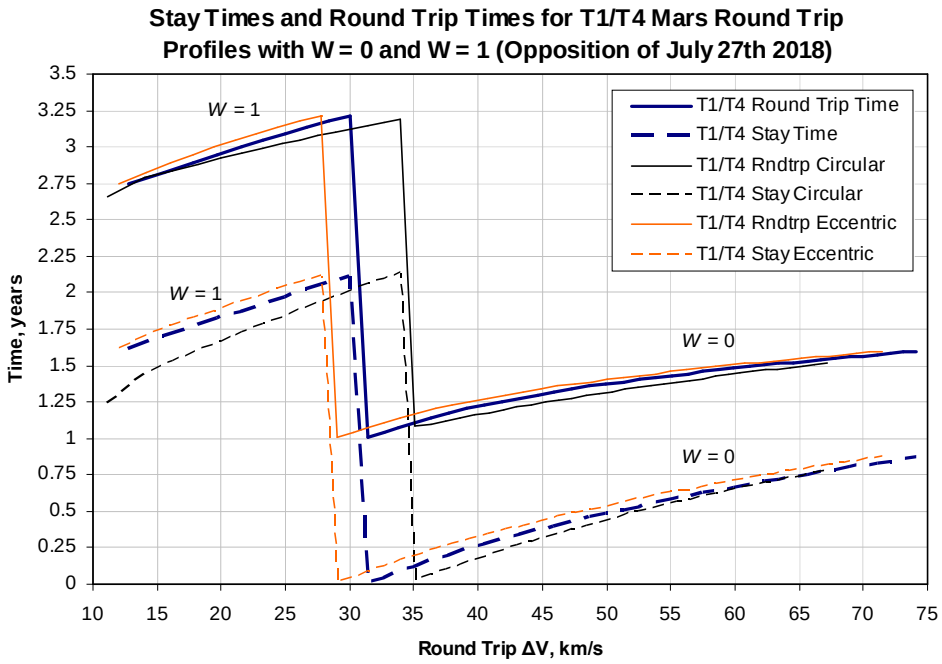

Figure 12. T1/T4 total trip and stay times as a function of the total mission ΔV for real orbits compared to eccentric and circular orbits. Opposition of July 27th, 2018.

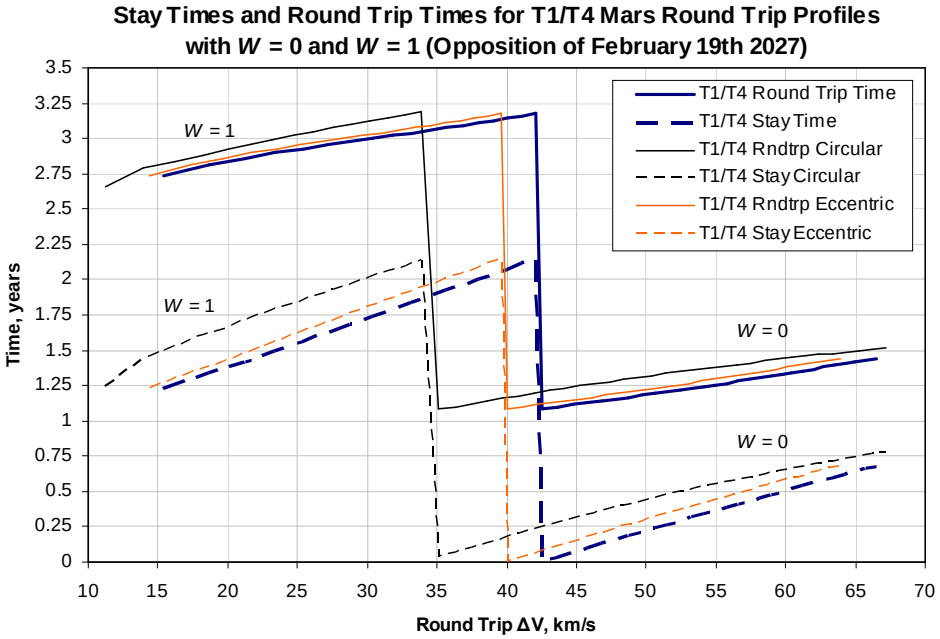

Figure 13. T1/T4 total trip and stay times as a function of the total mission ΔV for real orbits compared to eccentric and circular orbits. Opposition of February 19th, 2027.

Figure 14 shows more results in terms of differences between circular orbits and real orbits at two antipodal opposition dates (July 27th, 2018 and February 19th, 2027), for T1 outbound profiles. It shows the sensitivities of the results to real orbits, in particular the differences between circular and real orbits in terms of outbound transfer times as a function of total mission ΔV. Clearly, the results for circular orbits of the Earth and Mars fall in between the results for the opposition of July 27th, 2018 and those for the opposition of February 19th, 2027. In particular, compared to circular orbits, the situation is generally more favorable for the opposition of July 27th, 2018, and less

favorable for the opposition of February 19th, 2027. This is due to the fact that at the July 27th, 2018 opposition the Earth and Mars are closest, whereas at the February 19th, 2027 opposition they are farthest.

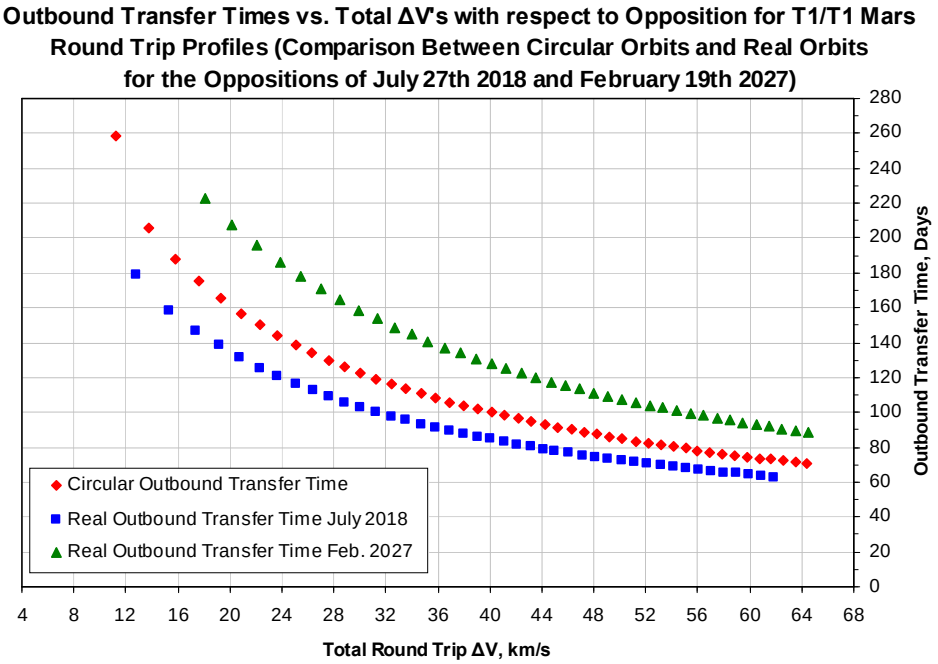

Figure 14. T1/T1 profile. Outbound transfer time vs. total round trip Δ*V*. Differences between circular and real orbits for two oppositions.

Figure 15 shows the interplanetary train schedule plots for real orbits, referred to T1/T1 profiles at the July 27th 2018 opposition timeframe. The results are different from the cases with circular coplanar orbits, since this time the eccentricities and plane change Δ*V*'s have been included. The plot also has additional features: the orange and blue curves represent the splits between the departure Δ*V*'s, the arrival Δ*V*'s, and the plane change Δ*V*'s. Related to this feature is the addition of markers on the black curves (which are selected cases) that represent the relative proportions between the departure, arrival, and plane change Δ*V*'s for each leg. There are therefore three segments for each leg, which, however, do not have a real physical meaning, in that nothing "physical" happens at the times indicated by their extremes. They are just a visual expedient to show the proportions between individual Δ*V*'s.

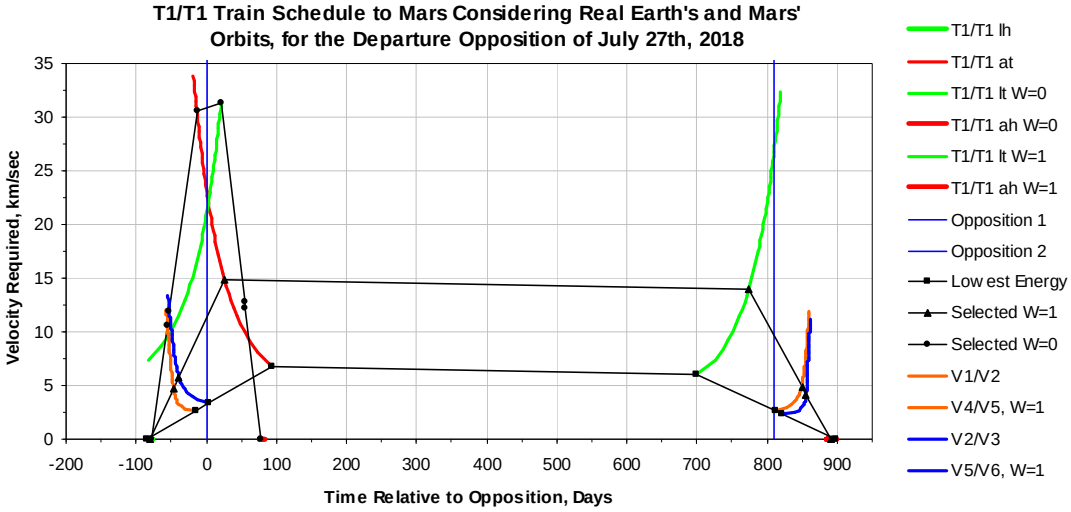

Figure 15. T1/T1 real ITS profiles for the departure opposition of July 27th, 2018.

VII. Architecture Design for a Selected Rapid Round Trip Mission

A. Mission Selection

A representative rapid round trip mission that could be accomplished by a crew was picked, and an assessment of the type of propulsion system, the propellant mass, and the number of launches required to accomplish such mission was done. The chosen candidate was a rapid T1/T4 mission profile at moderate energy, for the opposition timeframe of February 19th 2027, which represents the farthest approach between the Earth and Mars and therefore a designing case. The mission that was chosen, shown in Fig. 16, has the following astrodynamical specifications:

- Round trip profile: T1/T4 (direct/indirect)
- *W*=0 (rapid round trip)
- Opposition date timeframe: February 19th, 2027
- Earth departure date: November 27th, 2026
- Mars arrival date: March 29th, 2027
- Mars departure date: April 23rd, 2027
- Earth arrival date: January 8th, 2028
- Total round trip time: 406.80 days = 1.11 years
- Stay time: 25.12 days = 0.069 years
- Outbound transfer time: 122.35 days
- Return transfer time: 259.33 days
- Closest approach to the Sun: 0.5275 AU (it occurs at return). For comparison, Venus' semimajor axis is 0.7233 AU, and Mercury's semimajor axis is 0.387 AU.

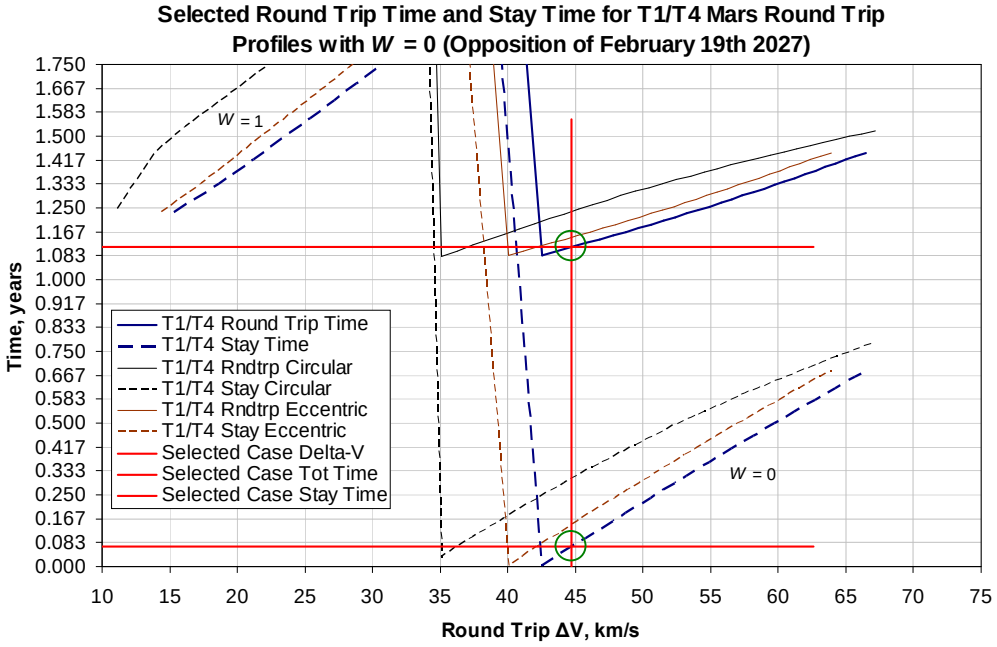

Figure 16. T1/T4 mission profile selection, for the departure opposition of February 19th, 2027.

The transfer arcs and the stay arc can be seen in Fig. 17. The line that is half solid and half dashed (1st and 3rd quadrants) represents the line of nodes of Mars' orbit (solid for the ascending node, and dashed for the descending node). The Figure clearly shows that the return trajectory goes inside the Earth's orbit, and that the stay time occurs on the portion of Mars' orbit above the ecliptic plane. It can also be seen that the stay period occurs when the Earth is still in front of the Sun (see hollow blue triangles), making communications between the two planets much easier. The mission occurs approximately during the second half of Solar Cycle 25 (between maximum and minimum)(see for example www.nasa.gov).

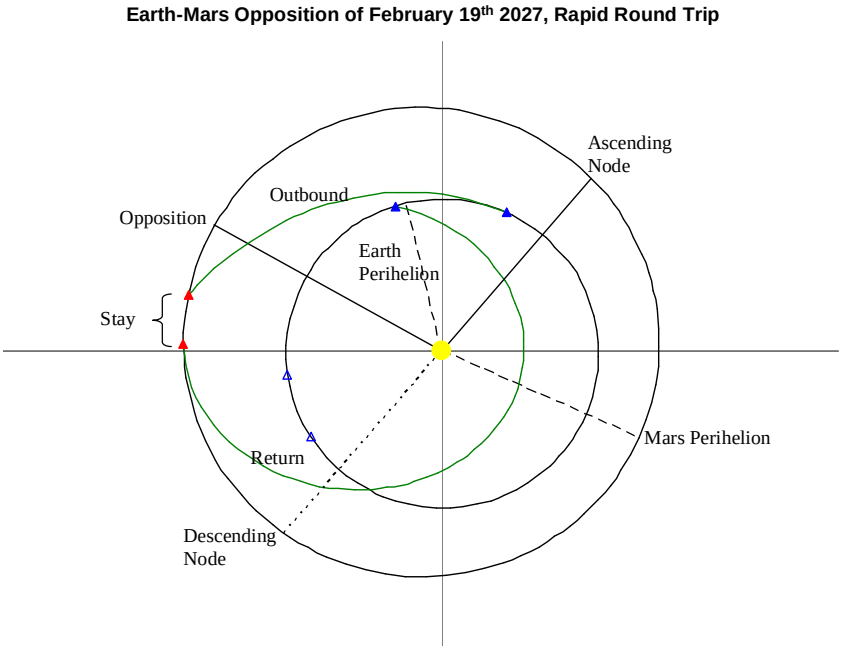

Figure 17. Transfer arcs for the selected T1/T4 mission profile, for the departure opposition of February 19th, 2027.

This mission was chosen because it has a short total round trip time, of only 1.1 years, and a short stay time, of only 25 days. This kind of mission could save in resources and costs compared to a long duration round trip, while still allowing humans to go to Mars for few weeks. It is important to point out that only the vehicle that carries the crew is required to comply with the selected mission profile. Any components of the mission that can be sent one synodic period in advance to Mars will travel on a low-energy trajectory which has not been extensively analyzed at this point.

B. Mission Architecture Design

The launch site from Earth has been assumed to be Kennedy Space Center, at 28.5º latitude north. In the study, additionally, the actual hyperbolic ΔV's necessary to escape from, and rendezvous with, Earth and Mars have been considered, instead of the heliocentric ΔV's written above, to give a more realistic estimate of the amount of propellant needed in those phases.

The main characteristics of the rapid round trip mission that has been designed are the use of chemical propulsion for all phases, use of a pre-deployed Earth return Vehicle (ERV), use of In-Situ Resource Utilization (ISRU) on Mars, and Aerocapture at Mars. The crew has been assumed to be of 4 people.

In order to characterize the necessary initial mass in LEO (IMLEO) and size the launch vehicle, the mission design was divided in eight separate phases, which occur in sequence. Such phases are the following:

1. Earth launch
2. Trans-Mars Injection (TMI)
3. Mars orbit insertion (MOI)
4. Mars landing
5. Mars launch
6. Trans-Earth Injection (TEI)
7. Earth capture
8. Earth landing

For the design, the above phases were considered backwards (as it is usually done in a rocket science problem), by first estimating the mass of the Earth Reentry Capsule (ERC) and then by assuming that such mass is the payload for the previous phase, and so on for all phases, until all the masses required for the mission are calculated. To perform these critical calculations, the rocket equation was used. In particular, the form of the equation that was used included the gravity loss term (where applicable) and the results in term of ΔV were corrected by drag and steering loss factors as well (where applicable). Also, the planets' (Earth's and Mars') contributions of the surface

speeds at the launch sites were accounted for when calculating the ΔV's. Such contributions were favorable since prograde orbits were considered. The rocket equation, in the most general form that was used, is written below:

$$R = e^{\frac{\Delta V + g\cos(\vartheta)\cdot t_b}{I_{sp} g_0}} \tag{21}$$

where:

- R is the mass ratio, equal to m_0/m_b
- m_0 is the initial mass, equal to $m_L+m_S+m_P$
- m_b is the burnout mass, equal to m_L+m_S
- m_L is the payload mass
- m_S is the structural mass
- m_P is the propellant mass
- ΔV is the change in velocity that needs to be provided
- I_{SP} is the specific impulse of the vehicle or stage
- g_0 is the gravitational acceleration at the Earth's surface, equal to 9.807 m/s^2
- g is the local gravitational acceleration at the location of the maneuver
- ϑ is the angle between the vehicle's velocity direction and the vertical
- t_b is the burn time

To get familiar with the global picture of this design, the overall mission sequence is presented in Fig. 18, which has a similar format (but different message) to that adopted in Ref. 7; the Figure shows the launch campaign and all the phases of the mission (both cargo and crewed). In particular, it can be seen that a cargo mission is launched in the 2024 timeframe (about 3 months before the opposition of January 16th, 2025), nearly one synodic period before the crew departure from Earth, which instead occurs on November 27th, 2026.

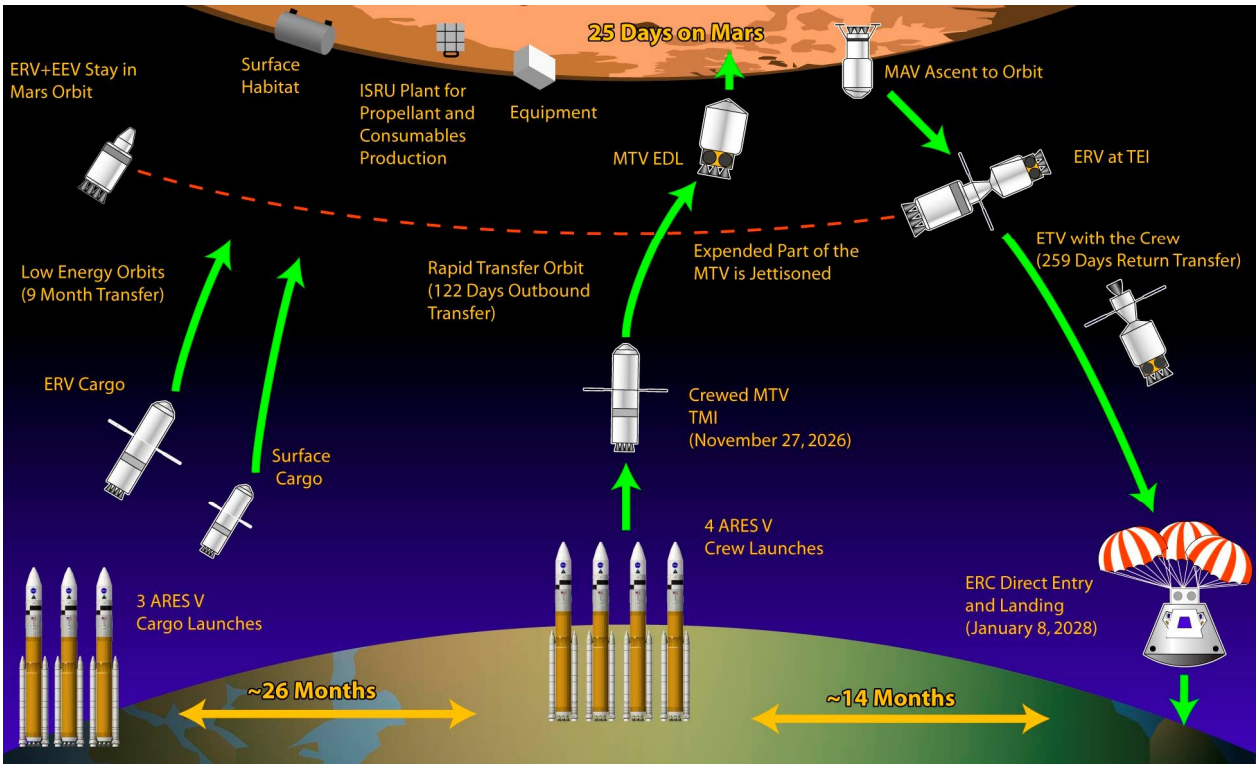

Figure 18. Selected RRT mission sequence.

In particular, it is assumed that the crew makes an aerocapture maneuver at Mars using a rigid biconic aeroshell, and inserts into an elliptical post-aerocapture 45 x 500 km orbit (shown in Fig. 19), similar to what is proposed in Refs. 8 and 9. After about 1 hour, the crew circularizes into a 500 km orbit by raising the periareion altitude with a

propulsive trim maneuver at apoareion (104 m/s), and about 2 hours later makes a deorbit burn (396 m/s) and descends.

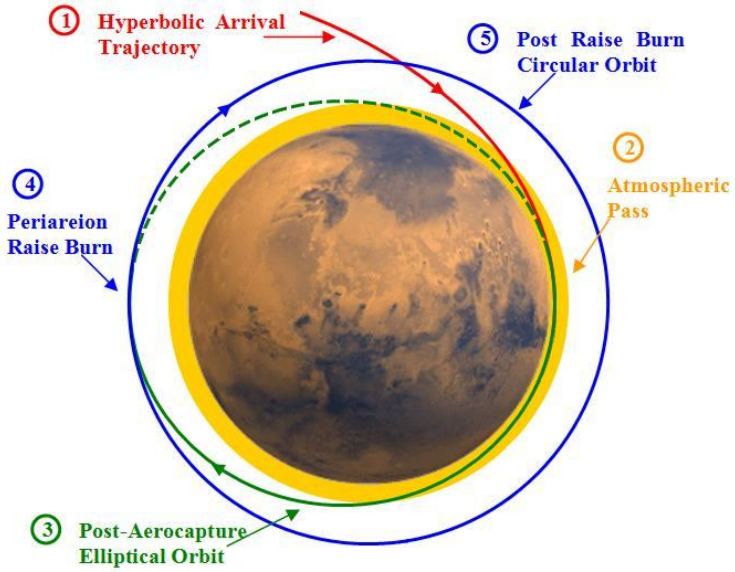

Figure 19. Mars aerocapture sequence.

It has been calculated that this maneuver produces an acceptable level of g's of acceleration on the crew. This strategy is more favorable than a capture into a highly elliptical orbit (which, however, would reduce the g-load slightly), because that orbit would have a longer period (equal or greater than a Martian sol, 24.62 hours) which would eat out time from the stay on the surface, already short enough. Conceptually different alternatives to this choice would be aerobraking and direct entry. These two options would be unfavorable for the current kind of mission (rapid round trip with short stay), since aerobraking would require too much time (at least few weeks, likely few months), and direct entry would create too many g's of acceleration on the crew.[8-11] The definitions of aerobraking and direct entry are given in Refs. 9 and 10. More details about the single phases of the mission are presented in Ref. 5.

The main result in terms of radiation protection is the use of aluminum to protect a cylindrical shelter 2 m in diameter, 2.5 m tall, and 4 cm thick, having a total mass of 2.2 mT. The calculations made for this assessment were based on Refs. 9, 10, and 12.

C. Total Number of Launches

The IMLEO for the crew mission is 662.16 mT. Instead, for the cargo mission (all components that are sent to Mars one synodic period in advance) only a rough assessment of the IMLEO was made. The elements that are sent to Mars in advance are: Earth return vehicle (218.84 mT), Crew surface equipment (10 mT), ISRU plant (7 mT), Liquid hydrogen: 2.83 mT. LH2 is used by the ISRU plant to produce not only LOX and CH4 propellants, but also breathable oxygen and drinkable water. For comparison, NASA DRM-3 uses instead 5 mT of hydrogen.[13]

To obtain the corresponding masses in LEO for the cargo mission (both the orbit payload and the surface payload), a crude comparison with NASA's DRM-3 was made in terms of gear ratios, which are defined as the ratios between the LEO mass and the actual mass delivered to Mars. By applying the same gear ratios to our mission (2.04 for the orbital payload and 3.35 for the surface payload) the result is an IMLEO of 447.4 mT for the ERV and of 66.4 mT for the surface payload, for a total IMLEO of the cargo mission of 513.8 mT. It is assumed that these results are comprehensive of all orbital maneuvers made during the mission, including plane changes.

To decide how many launches from Earth are needed to deliver the required masses to LEO, the method was to pick few selected representative vehicles and assume to use those for the mission. The vehicles that were considered are the Saturn V, the Ares V, and an arbitrary evolved expendable launch vehicle (EELV), for example an evolved Delta IV or Atlas V. The class (i.e., LEO capability) of these three vehicles and their required number of launches are presented in Table 1:

Table 1. Three representative launch vehicles and their required number of launches.

	Class (LEO Capability)(mT)	Number of Launches in Advance (Cargo Mission)	Number of Launches of the Crew Mission	Total Number of Launches
Saturn V	119	5	6	11
Ares V	188	3	4	7
EELV	90	6	8	14

Of these results, the number of launches required for the crew mission is a fairly accurate value, whereas the number of launches for the cargo mission is only an estimate.

For the crew mission, the theoretical heliocentric ΔV required is 44.7 km/s, whereas in reality, by considering the actual hyperbolic passages to and from the planets, such value becomes about 39 km/s. The total required crew mission ΔV, including not only the hyperbolic passages, but also the ΔV's for launch and landing and the ΔV's for the deep space plane change maneuvers, is about 58 km/s. However, since some of the maneuvers are done by aero assist at the planets, the actual total propulsive ΔV required by the crew mission from LEO is 22.6 km/s (it does not include the Earth launch ΔV).

D. Comparison with the NASA Mars Reference Missions.

This section compares the main characteristics of the selected rapid round trip mission with the three NASA design reference missions: DRM-1, DRM-3, and DRA-5. Table 2 shows the astrodynamical specifications of the RRT mission and compares them with NASA. It is clear from the table that all three of the NASA baseline architectures are long-duration missions with a long stay on the surface. The typical stay time for those missions is about 600 days, the transfer times are of about 180 days each way, and the total mission duration is of 2.63 years. For the current RRT mission, the stay time is of 25 days, the transfer times are of 122 and 259 days respectively, and the total mission duration is 1.11 years.

Table 2. Astrodynamical specifications comparison between the selected RRT and the NASA Mars Reference Missions.

	Units	T1/T4, RRT	NASA DRM-1	NASA DRM-3	NASA DRA-5
Round trip profile	-	T1/T4	Very similar to T1/T1	Very similar to T1/T1	Very similar to T1/T1
***W* =**	-	0	1	1	1
Opposition date	-	February 19 2027 (unfav.)	January 29 2010 (unfav.)	January 29 2010 (unfav.)	Early 2030's (fav.)
Total heliocentric Δ*V* (patched)	m/s	44,737	-	-	-
Earth departure Δ*V* (helioc.)	m/s	6,845	-	-	-
Out plane change Δ*V* (helioc.)	m/s	1,052	-	-	-
Mars arrival Δ*V* (helioc.)	m/s	12,983	-	-	-
Mars departure Δ*V* (helioc.)	m/s	6,034	-	-	-
Ret. plane change Δ*V* (helioc.)	m/s	1,506	-	-	-
Earth arrival Δ*V* (helioc.)	m/s	16,317	-	-	-
Outbound transfer time	days	122	180	180	180
Stay time	days	25	600	600	545
Stay time	years	0.07	1.64	1.64	1.49
Return transfer time	days	259	180	180	180
Total round trip time	days	407	960	960	905
Total round trip time	years	1.11	2.63	2.63	2.48
Outbound arc on ecliptic	º	12.11	-	-	-
Outbound arc off ecliptic	º	90	-	-	-
Inclination wrt Mars orbital plane	º	-1.851	-	-	-
Return arc on Mars orbit plane	º	199.09	-	-	-
Return arc off Mars orbit plane	º	90	-	-	-
Closest approach to the Sun	AU	0.528	1	1	1

Table 3 shows the main differences in terms of mission architecture between the selected RRT mission and the NASA missions. The main differences with DRM-1 and DRM-3 are in the IMLEO and in the total propellant mass. The RRT clearly needs much more propellant than the other two, given the higher mission ΔV's. As for the DRA-5, comparisons are harder since in its mission report multiple cases are compared but no one in particular is selected. However, in this research it was assumed that DRA-5 uses a nuclear thermal propulsion system, since it seems to be

slightly favored by NASA. Another difference is the amount of landed mass on Mars: for the short stay mission, such mass is clearly smaller. Additionally, it is interesting to compare the number of launches necessary for each mission architecture: both the RRT mission and the DRA-5 mission use the Ares V vehicle. However, there is dissimilarity in the assumed payload to LEO capability: 188 mT for the current mission, in agreement with the value reported on the official NASA website, against 131 mT used in the DRA-5 report.

Table 3. Mission architecture comparison between the selected RRT and the NASA Mars Reference Missions.

	Units	T1/T4, RRT	NASA DRM-1	NASA DRM-3	NASA DRA-5
N. of crew members	-	4	6	6	6
Average crew member mass	kg	75	83	83	-
Consumables + life support sys. (includes subsystem dry mass)	kg	9,882	19,000	9,768	-
Number of transit habitats (Transhabs)	-	1 (same one for TMI, Surface, and TEI)	2 (one for TMI and Surface, and one for TEI)	2 inflatable (one for TMI and Surface, and one for TEI)	Not specified (likely 2)
Total number of habitats	-	2 (1 inflatable habitat sent to surface)	3 (1 habitat sent to surface)	3 (1 inflatable habitat sent to surface)	Not specified (likely 3)
Transhab size (diam. x length)	m	6 x 6	7.5 x 7.5	9.5 x 9.7	-
Earth Launch site latitude	º N	28.50	-	-	-
Total IMLEO	mT	1,176.00	850.00	480.00	849.00
Mass landed on Mars with crew	mT	39.58	60.71	35.15	-
Useful mass landed with crew	mT	20.06	56.04	30.94	-
Total Mass landed on Mars	mT	61.48	245.00	95.95	-
Total useful mass landed	mT	39.89	112.29	71.18	-
Is ISRU used?	-	Yes; H2 brought from Earth in advance	Yes; H2 brought from Earth in advance	Yes; H2 brought from Earth in advance	Yes; H2 brought from Earth in advance
ISRU plant mass (including any LH2 brought from Earth)	mT	9.83	21.80	20.80	-
Launch vehicle class	mT	188	240	80	131
N. of launches in advance	-	3	3	4	5
N. of launches at the crew's opposition	-	4	1	2	4
N. of launch vehicles needed	-	7	4	6	9
Propulsion system type	-	All chemical	NTR (only for TMI); Chemical	NTR (only for TMI); Chemical	NTR (only for TMI); Chemical
TMI propellant type	-	LOX/LH2	NDR + LH2 (nuclear)	NDR + U, Zr, Nb + LH2 (nuclear)	NDR + U, Zr, Nb + LH2 (nuclear)
TEI propellant type	-	LOX/CH4	LOX/CH4	LOX/CH4	LOX/CH4
MDV/MAV propellant type	-	LOX/CH4	LOX/CH4	LOX/CH4	LOX/CH4
Propellant mass needed (excluding launch from Earth)	mT	814	334	197	-
Total propellant mass needed	mT	18,566	-	-	-

As a consequence, there is some dissimilarity in the number of launches as well, since the RRT mission uses 7 whereas the DRA-5 uses a total of 9. It was calculated that if the payload capability for the current mission was also 131 mT, the total number of launches would go up to 9 as well, like the value in DRA-5. As a note, DRA-5 considers also a completely chemical mission alternative, and in that case, the total number of launches of the Ares V is 12, definitely greater than 7. Clearly, on one hand the current RRT mission has an advantage in terms of consumables and equipment needed on the surface, whereas on the other hand it has a mass penalty given by the great amount of propellant needed by the chemical propulsion system. As another interesting note, the Augustine Commission's report[7] considers 8 Ares V (with an assumed capability of 160 mT) launches plus 1 Ares I launch.

As for DRM-1 and DRM-3, there are slightly more similarities in terms of number of launches, but still those missions clearly use less: DRM-1 uses only 4 launches of a 240 tonnes class vehicle, whereas DRM-3 uses only 6 launches of an 80 tonnes class vehicle. The main reason for this difference is that the ΔV requirements considered by NASA are smaller than those for the RRT mission, producing a less stringent propellant mass demand. However, this does not fully explain the difference between the two early NASA architectures and that of the newer DRA-5. A

rationale for this fact could be that the early architecture studies might have underestimated some of the important masses involved, like for example those for the radiation protection system, the power system, the aeroshell used for Mars aerocapture and descent, and the propellant needed for the deep space maneuvers.

VIII. Conclusions

The presented research consists of two parts: an astrodynamics study and a systems engineering study. The astrodynamics study addressed the problem of applying the round trip constraint equations to Earth-Mars missions, for which the real orbits of the Earth and Mars were considered as opposed to circular coplanar orbits. Additionally, interplanetary train schedule (ITS) plots for real orbits were created and compared to those for circular coplanar orbits.

The profiles that were considered for this comparison are T1/T1 and T1/T4, and the opposition dates that were analyzed are July 27th, 2018 and February 19th, 2027, because they represent two examples of closest and farthest approach of the Earth and Mars, respectively. An iterative method was used to obtain the desired transfer arc types and at the same time calculate the exact departure dates from both the Earth and Mars.

The main results of this study are that for the opposition of July 27th, 2018 and for both T1/T1 and T1/T4 profiles, the transfer times can be shorter than for circular orbits by up to 4 weeks at outbound and by up to 6 weeks at return. For the opposition of February 19th, 2027 and for both T1/T1 and T1/T4 profiles, the transfer times can be longer than for circular orbits by up to 6 weeks. Another important difference with circular orbits is that for the opposition of February 19th, 2027, rapid T1/T1 round trip missions are not possible using elliptical transfer orbits, given the farther distance between the Earth and Mars. In this case, only hyperbolic transfers are allowed (but such case was not studied).

The second part of this research is a systems engineering study. A representative W=0 (rapid round trip) mission was selected and developed further. The mission that was chosen has a T1/T4 profile and departs near the opposition of February 19th, 2027, in particular on November 27th, 2026; the total round trip time is 406.8 days (1.11 years) and the stay time is 25.1 days; the return to Earth occurs on January 8th, 2028. This particular mission has its closest approach to the Sun at 0.5275 AU (at return).

For this selected mission, an opportune transportation architecture has been designed to fit in the best way possible the specifications of the mission itself. In particular, it has been chosen that for this mission only chemical propulsion would be used, since currently it is the only viable technology. Also, the system uses a pre-deployed cargo that launches towards Mars one synodic period in advance on a low-energy trajectory. The crew, made of 4 people, launches instead on the selected high-energy mission profile. Additionally, Mars aerocapture for the crewed vehicle and ISRU are employed as well. This is a combination of options that has never been developed before, as shown by the trade tree in Ref. 9. The mission has been divided in several segments, and the masses and sizes of the transportation elements in each segment have been calculated.

The final result is that only 7 launches of a heavy lift vehicle of the capability of the Ares V (188 mT) are needed to realize the mission, in particular 3 launches for the cargo mission and 4 launches for the crew mission. NASA DRM-1 and DRM-3 use less launches but they assume nuclear propulsion (which is not yet a consolidated reality), and they neglect to include some of the masses such as those of the radiation protection system and the power system. In addition, DRM-1 assumes the use of a 240 mT class heavy lift vehicle. As for DRA-5, NASA assumes that 9 launches of a 131 mT class Ares V vehicle are needed to accomplish the mission, which also uses nuclear propulsion. Therefore, the final conclusion is that the short stay mission at high transfer energy can certainly compete with the reference missions in terms of practicality, number of launches, and masses involved. The rapid round trip mission is definitely affordable and achievable with current technologies.

Acknowledgments

The authors thank the University of Southern California, in particular the following professors of the Astronautical Engineering Department: Dan Erwin, Mike Gruntman, and Joseph Kunc and the following professors of the Aerospace and Mechanical Engineering Department: Firdaus Udwadia and Paul Newton, for their support and guidance. N. Sarzi Amade' greatly thanks Microcosm, Inc., for allowing the realization of this research.

References

[1]Hoffman, S. J., and Kaplan, D.I., (eds.), **"**Human Exploration of Mars: The Reference Mission of the NASA Mars Exploration Study Team," NASA Special Publication 6107, Lyndon B. Johnson Space Center, Houston, TX, July 1997.

[2]Wertz, J. R., "Interplanetary Round Trip Mission Design," 54th International Astronautical Congress, IAC-03-Q.4.06, Bremen, Germany, Sept. 29-Oct. 3, 2003.

[3]Wertz, J. R., "Rapid Interplanetary Round Trips at Moderate Energy," 55th International Astronautical Congress, IAC-04-Q.2.a.11, Vancouver, BC, Canada, Oct. 4-8, 2004.
[4]Seidelmann, P. K., (ed.), *Explanatory Supplement to the Astronomical Almanac*, University Science Books, Mill Valley, CA, 2006.
[5]Sarzi Amade', N., "Mars Rapid Round Trip Mission Design," Ph.D. Dissertation, University of Southern California, Los Angeles, CA, August 2010.
[6]Wertz, J. R., *Mission Geometry; Orbit and Constellation Design and Management*, Space Technology Library, Microcosm Press and Kluwer Academic Publishers, El Segundo, CA, and Dordrecht, The Netherlands, 2001.
[7]Review of U.S. Human Spaceflight Plans Committee, "Seeking a Human Spaceflight Program Worthy of a Great Nation," Washington, DC, October 2009.
[8]Wright, H. S., et al., "Mars Aerocapture System Study," NASA/TM-2006-214522, November 2006.
[9]Drake, B.G., (ed.), "Human Exploration of Mars Design Reference Architecture 5.0: Addendum," NASA/SP-2009-566-ADD, NASA Headquarters, July 2009.
[10]Rapp, D., *Human Missions to Mars. Enabling Technologies for Exploring the Red Planet*, Springer and Praxis Publishing, Chichester, England, 2008.
[11]Alemany, K., Wells, G., Theisinger, J., Clark, I., and Braun, R., "Mars Entry, Descent, and Landing Parametric Sizing and Design Space Visualization Trades," AIAA Astrodynamics Specialist Conference, AIAA 2006-6022, Keystone, CO, August 2006.
[12]Zubrin, R.M., Baker, D.A., and Gwynne, O., "Mars Direct: A Simple, Robust, and Cost Effective Architecture for the Space Exploration Initiative," AIAA-91-0328, 1991.
[13]Drake, B.G., (ed.), "Reference Mission Version 3.0. Addendum to the Human Exploration of Mars: The Reference Mission of the NASA Mars Exploration Study Team," NASA/SP-6107-ADD, Lyndon B. Johnson Space Center, Houston, TX, June 1998.